

# ZnO thin film nanostructures for hydrogen gas sensing applications

Husam S. Al-Salman<sup>a,b,\*</sup>, M.J. Abdullah<sup>a</sup>, Naif Al-Hardan<sup>c</sup>

<sup>a</sup>*School of Physics, Universiti Sains Malaysia, 11800 Penang, Malaysia*

<sup>b</sup>*Department of Physics, College of Science, University of Basrah, Basrah, Iraq*

<sup>c</sup>*Ministry of Science and Technology, Baghdad, Iraq*

Available online 23 October 2012

## Abstract

A ZnO thin film-based gas sensor was fabricated using a SiO<sub>2</sub>/Si substrate with a platinum comb-like integrated electrode and heating element. The structural characteristics, morphology, and surface roughness of the as-grown ZnO nanostructure were investigated. The film revealed the presence of a *c*-axis oriented (002) phase with a grain size of 20.8 nm. The sensor response was tested for hydrogen concentrations of 50, 70, 100, 200, 400, and 500 ppm at the optimum operating temperature of 350 °C. The sensitivities towards 50 and 200 ppm of hydrogen gas at 350 °C were approximately 78% and 98%, respectively. A linear response was observed for hydrogen concentrations within the range of 50 ppm–200 ppm. These results demonstrated the potential application of the ZnO nanostructure for the fabrication of cost-effective and high-performance gas sensors.

© 2012 Elsevier Ltd and Techna Group S.r.l. All rights reserved.

**Keywords:** D. ZnO; E. Sensors; RF sputter

## 1. Introduction

Pure hydrogen gas (H<sub>2</sub>) is considered to be non-toxic, but it can cause suffocation by reducing the relative oxygen concentration in an enclosed area; the oxygen deficiency could cause rapid breathing, diminished mental alertness, impaired muscular coordination, and fatigue, which can all lead to prostration, unconsciousness, convulsions, coma, and death [1]. Thus, small leaks of H<sub>2</sub> in an enclosed area may lead to immediate unconsciousness at oxygen concentrations less than 12%, thereby increasing the risk of asphyxiation as well as that of combustion and explosion [1]. Therefore, a reliable and cost-effective hydrogen gas sensor for the timely detection of conspicuous H<sub>2</sub> in the environment needs to be developed for safety and economic reasons.

Semiconductor oxides such as SnO<sub>2</sub>, Fe<sub>2</sub>O<sub>3</sub>, Ga<sub>2</sub>O<sub>3</sub>, and Sb<sub>2</sub>O<sub>3</sub> are widely used to detect inflammable and toxic gases [2]. However, the distinct advantages of the ZnO nanostructure such as its chemical sensitivity to several gases, high chemical stability, non-toxicity, and low cost [3]

have motivated numerous researchers to investigate the applications of its gas response. ZnO has been successfully employed to detect various gases, including H<sub>2</sub>, NO<sub>2</sub>, O<sub>2</sub>, CH<sub>3</sub>CH<sub>2</sub>OH, NH<sub>3</sub>, liquefied petroleum gas [4], and trimethylamine [5]. Thus, the cost, compactness, reliability, and selectivity must be considered in the fabrication of nanosensor devices, aside from the different technical requirements.

In this work, a ZnO nanostructure-based gas sensor was synthesized on SiO<sub>2</sub>/Si (100) with a platinum comb-like integrated electrode and heating element using a RF-magnetron sputtering. The ZnO based gas sensor was characterized by X-ray diffraction (XRD) and field emission scanning electron microscopy (FESEM). The sensitivity of the gas sensor towards H<sub>2</sub> was tested in temperature range of 250 °C–400 °C.

## 2. Experimental

The N-type (100) silicon wafer (8 mm × 10 mm) was cleaned by the standard (RCA) method. The wafer was then heated at 1100 °C for 5 h in a tube furnace under wet air to produce a 1.2 μm-thick layer of SiO<sub>2</sub>. Photolithography was performed to produce a Pt integrated electrode

\*Corresponding author at: School of Physics, Universiti Sains Malaysia, 11800 Penang, Malaysia. Tel.: +60 17 8016079.

E-mail address: [husam.shakir@yahoo.com](mailto:husam.shakir@yahoo.com) (H.S. Al-Salman).

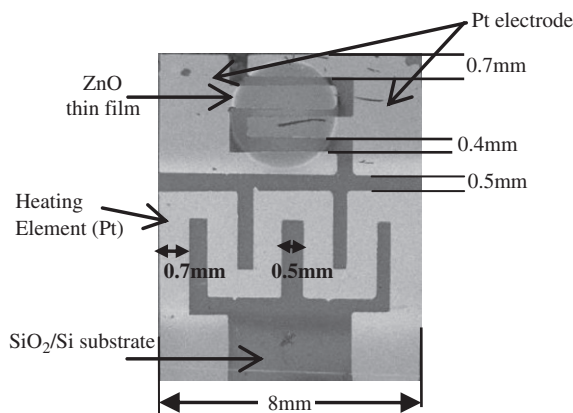


Fig. 1. SEM image of the fabricated device for hydrogen sensing measurement.

and heating element ( $\sim 200$  nm) with a Ti adhesion-promotion layer ( $\sim 40$  nm) on a  $\text{SiO}_2/\text{Si}$  substrate. Pt and Ti were deposited using an Edwards A500 RF-magnetron sputtering unit. The same sputtering unit was used to prepare the circular ZnO nanostructure-based gas sensor with a radius of 1.2 mm and a thickness of 260 nm using a base pressure of  $2 \times 10^{-5}$  mbar and a power of 150 W. However, during the sputtering process, the temperature rose to approximately  $60^\circ\text{C}$  because of self-heating.

The film was then heat-treated at  $600^\circ\text{C}$  in air for 1 h. The heating element was then coated with 150 nm of  $\text{SiO}_2$  to increase its lifetime and eliminate its interaction with the tested gases. Fig. 1 shows the top view of the fabricated hydrogen sensor with total dimensions of  $8\text{ mm} \times 10\text{ mm}$ .

The current–voltage ( $I$ – $V$ ) characteristics of the Pt/ZnO/Pt device were determined by a DC voltage sweep using a Keithley 237 source-measure unit. The gas measurement units were controlled by a PC through a GPIB interface, and the LabVIEW (version 8.5) software was used for data acquisition. The gas sensing measurements were performed at temperatures within the range of  $250^\circ\text{C}$ – $400^\circ\text{C}$ .

The temperature was varied and controlled by changing the applied voltage to the Pt heating element using a DC-regulated power supply. The temperature was measured by a Pt-100 RTD (with a ceramic envelope) that was connected to a Keithley 2100 DMM.

XRD analysis was performed in the range of  $20^\circ$ – $60^\circ$  using a PANalytical X'Pert PRO X-ray diffractometer (MRD PW3040; Almelo, Netherlands) with  $\text{CuK}\alpha$  radiation ( $\lambda = 1.541 \text{ \AA}$ ). FESEM was performed using a Leo-Supra 50VP microscope (Carl Zeiss, Germany). Atomic force microscopy (AFM; Dimension Edge, Bruker) in the Tapping mode as well as the NanoDrive dimension-edge-tapping image-processing software were used to measure the surface roughness of the film.

### 3. Results and discussion

The XRD diffraction pattern of the deposited ZnO film at room temperature is shown in Fig. 2. The ZnO film was

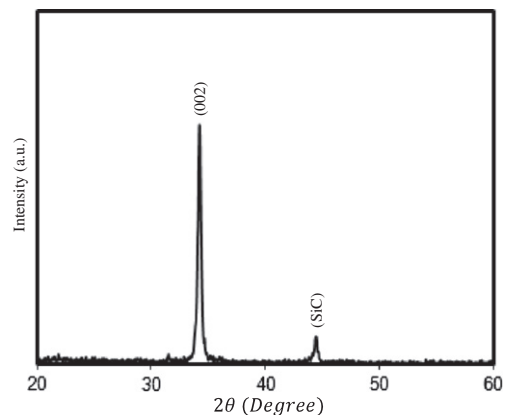


Fig. 2. X-ray diffraction pattern of the ZnO nanostructure on a  $\text{SiO}_2/\text{Si}$  substrate.

Table 1

Properties of the ZnO nanostructure deposited on a  $\text{SiO}_2/\text{Si}$  substrate by RF-magnetron sputtering.

Lattice parameter		Strain (%)	Grain size (nm)
a(Å)	c(Å)		
3.249	5.219	0.0021	20.8

found to be highly oriented along the  $c$ -axis and belongs to the (002) peak of the wurtzite structure with a lattice constant  $c = 5.219 \text{ \AA}$ . Thus, the film agrees with the standard data of ICDD 04-006-1673. The minor peak that was detected at  $44.5^\circ$  is attributed to the silicon carbide of the XRD sample holder [6].

The average grain size ( $D$ ) and strain ( $\varepsilon_{zz}$ ) of the ZnO nanostructure along the  $c$ -axis were calculated (Table 1) using the XRD data and the following equations [6,7]:

$$D = \frac{0.9 \lambda}{\beta \cos \theta} \quad (1)$$

$$\varepsilon_{zz} = \frac{c - c_o}{c_o} \times 100 \quad (2)$$

where  $\lambda = 1.541 \text{ \AA}$  is the wavelength of the  $\text{CuK}\alpha$  radiation,  $\beta$  denotes the half-width at half-maximum (HWHM) of the peak,  $\theta$  is the Bragg angle,  $c$  is the lattice constant of the ZnO film that was estimated from the XRD data, and  $c_o$  ( $5.207 \text{ \AA}$ ) is the standard lattice constant for unstrained ZnO. The obtained strain value was very low (0.002) as compared with the value estimated by Hassan et al. [6], who synthesized ZnO nanorods on Si substrate by microwave-assisted chemical bath deposition (CBD). The low strain value suggests the high quality of the film.

A typical FESEM image of the ZnO film is shown in Fig. 3, in which the film uniformity is clearly demonstrated. Fig. 4 depicts the AFM image of the ZnO film surface, which reveals a homogeneous surface with a roughness ( $R_{\text{rms}}$ ) of 1.97 nm.

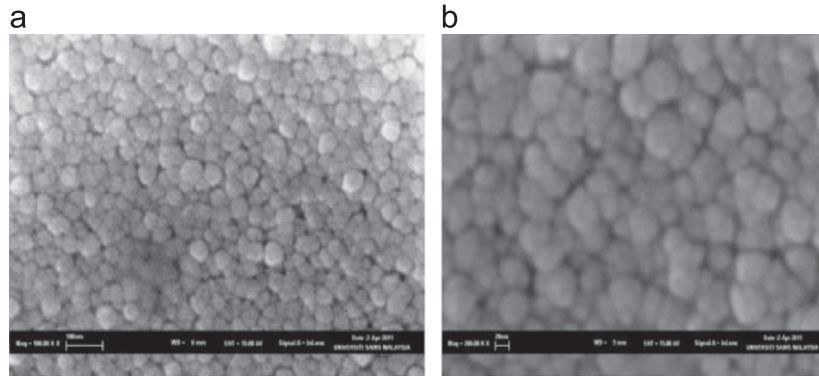


Fig. 3. FESEM image of the ZnO nanostructure on a SiO<sub>2</sub>/Si substrate: (a) 100kX and (b) 200kX.

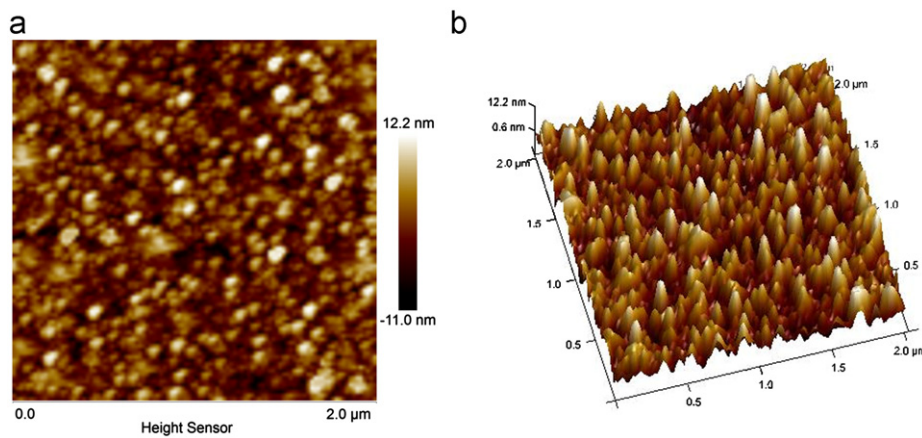


Fig. 4. AFM images (2  $\mu\text{m} \times 2 \mu\text{m}$ ) of the ZnO nanostructure on a SiO<sub>2</sub>/Si substrate ( $R_{\text{rms}}=1.97 \text{ nm}$ ): (a) 2D and (b) 3D.

The  $I$ – $V$  plot of the ZnO gas sensor showed a linear behavior, thereby indicating its ohmic characteristic at room temperature (not mentioned here).

The sensitivity of the sensor for 200 ppm of H<sub>2</sub> at different temperatures was measured and determined according to the following equation:

$$S(\%) = \frac{R_a - R_g}{R_a} \times 100 \quad (3)$$

where  $R_g$  and  $R_a$  are the resistances of the gas sensor in gas and air atmospheres, respectively. The sensitivity showed that the optimum operating temperature was 350 °C (Fig. 5).

The observed behavior can be explained by the activation of adsorbed oxygen species on the surface of the sample film [8].

The high sensitivity of the ZnO gas sensor that was obtained could be attributed to the nanostructure of the grains, which had a relatively large surface area [9].

The gas sensor response for different hydrogen concentrations (50 ppm–500 ppm) at the optimum operating temperature of 350 °C is presented in Fig. 6. The response repeatability of the gas sensor is depicted in the inset of Fig. 6 for 200 ppm of H<sub>2</sub>. The high reproducibility and

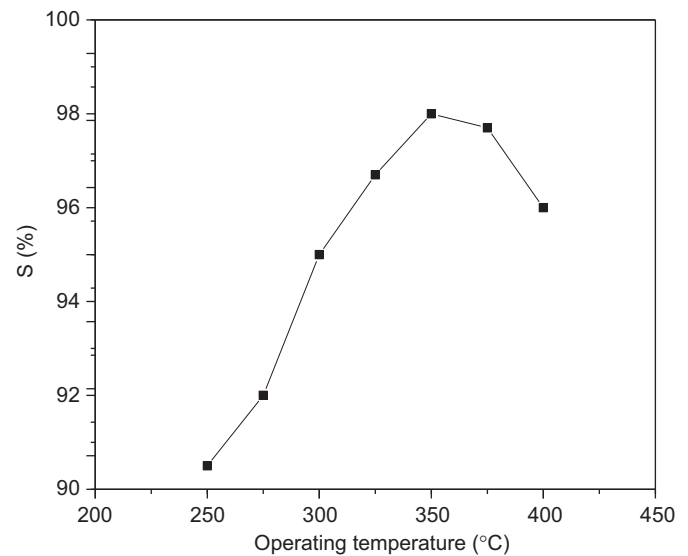


Fig. 5. Sensitivity of the ZnO gas sensor for 200 ppm of H<sub>2</sub>.

baseline stability of the sensor was observed with the repeated exposure and removal of hydrogen gas at an operating temperature of 350 °C. Therefore, the gas sensing capacity

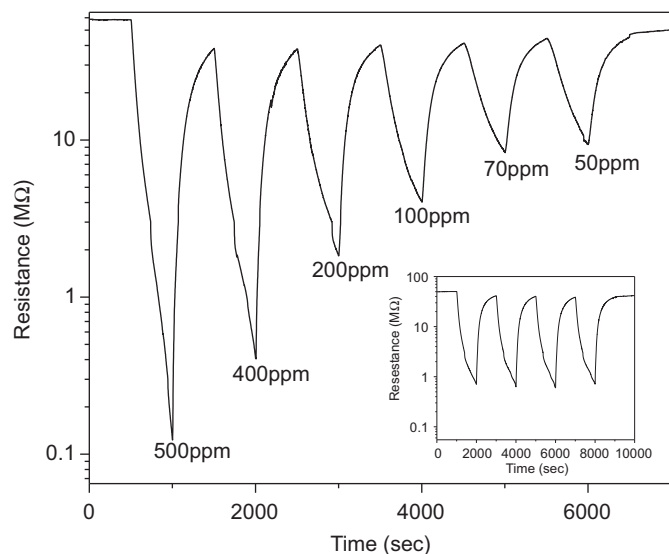


Fig. 6. Response of the ZnO gas sensor for different  $H_2$  concentrations at 350 °C. The inset shows the repeatability of the response for 200 ppm of  $H_2$ .

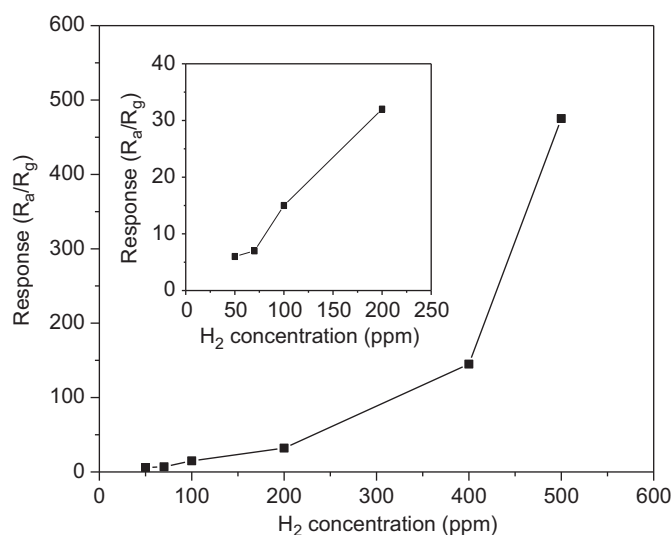


Fig. 7. Response of the ZnO gas sensor as a function of the  $H_2$  concentration at 350 °C.

is stable and the recovery abilities of the sensor were maintained even after several sensing cycles. The response of the gas sensor as a function of hydrogen concentration is shown in Fig. 7, in which a linear dependence can be observed at low concentrations (50 ppm–200 ppm) followed by high response rate at higher gas concentrations.

The  $H_2$  response ( $R_a/R_g$ ) of the ZnO gas sensor that was obtained in the present work was much higher as compared with the value estimated by Yanxia et al. [10] (response of  $\sim 2.46$  at 5000 ppm and 300 °C), who synthesized a ZnO thin film on sapphire by the pulsed laser deposition (PLD) technique.

#### 4. Conclusions

A nanostructured ZnO gas sensor was successfully synthesized with a platinum comb-like integrated electrode and heating element on an  $SiO_2/Si$  substrate by RF-magnetron sputtering. The XRD spectrum of the ZnO nanostructure showed the formation of a hexagonal structure belonging to the (002) phase with a grain size of 20.8 nm.

With the optimum operating temperature of 350 °C, the sensing characteristics of the gas sensor such as high sensitivity, excellent stability, and full recovery to the initial value of the sensor signal were observed. The Pt heating element had higher stability and a longer life time after it was coated with a  $SiO_2$  layer.

#### Acknowledgments

The authors would like to thank the Nano-Optoelectronics Research and Technology Laboratory (N.O.R.) of the School of Physics in the Universiti Sains Malaysia for the help they extended during the research.

#### References

- [1] College of the Desert, Energy Technology Training Center, Palm Desert, California, USA, Hydrogen Properties, Module 1 2001.
- [2] T.T. Trinha, N.H. Tuc, H.H. Lec, K.Y. Ryua, K.B. Lec, K. Pillai, J. Yia, Improving the ethanol sensing of ZnO nano-particle thin films—the correlation between the grain size and the sensing mechanism, *Sensors and Actuators B* 152 (2011) 73–81.
- [3] K. Liu, M. Sakurai, M. Aono, Pinecone-shaped ZnO nanostructures: growth, optical and gas sensor properties, *Sensors and Actuators B* 157 (2011) 98–102.
- [4] D. Calestania, M. Zhaa, R. Moscaa, A. Zappettinia, M.C. Carottab, V. Di Nataleb, L. Zanolitia, Growth of ZnO tetrapods for nanostructure-based gas sensors, *Sensors and Actuators B* 144 (2010) 472–478.
- [5] H. Nanto, H. Sokooshi, T. Kawai, Aluminum-doped ZnO thin film gas sensor capable of detecting freshness of sea foods, *Sensors and Actuators B* 14 (1993) 715–717.
- [6] J.J. Hassan, Z. Hassan, H. Abu-Hassan, High-quality vertically aligned ZnO nanorods synthesized by microwave-assisted CBD with ZnO–PVA complex seed layer on Si substrates, *Journal of Alloys and Compounds* 509 (2011) 6711–6719.
- [7] P. Prepelita, R. Medianu, B. Sbarcea, F. Garoi, M. Filipescu, The influence of using different substrates on the structural and optical characteristics of ZnO thin films, *Applied Surface Science* 256 (2010) 1807–1811.
- [8] X. Song, D. Zhang, M. Fan, A novel toluene sensor based on ZnO–SnO<sub>2</sub> nanofiber web, *Applied Surface Science* 255 (2009) 7343–7347.
- [9] N. Yamazoe, K. Shimano, Theoretical approach to the rate of response of semiconductor gas sensor, *Sensors and Actuators B: Chemical* 150 (2010) 132–140.
- [10] Y. Liu, T. Hang, Y. Xie, Z. Bao, J. Song, H. Zhang, E. Xie, Effect of Mg doping on the hydrogen-sensing characteristics of ZnO thin films, *Sensors and Actuators B* 160 (2011) 266–270.